RESEARCH REPOSITORY

Authors Version

Shafiei, M., Nourbakhsh, G., Arefi, A., Ledwich, G. and Pezeshki, H. (2019) Single iteration conditional based DSSE considering spatial and temporal correlation. International Journal of Electrical Power and Energy Systems, 107 . pp. 644-655.

Single Iteration Conditional Based DSE Considering Spatial and Temporal Correlation

Mehdi Shafiei, *Student Member, IEEE*, Ghavameddin Nourbakhsh, *Member, IEEE*, Ali Arefi, *Senior Member, IEEE*, Gerard Ledwich, *Senior Member, IEEE*, Houman Pezeshki, *Member, IEEE*

Abstract— **Active players are introducing significant challenges in electric distribution systems management. One of the key components of the distribution system management is state estimator. This paper proposes an efficient and accurate single iteration distribution system state estimation technique only requiring a limited number of real measurement units. A method based on conditional multivariate complex Gaussian distribution (CMCGD) is proposed to include spatial and temporal correlation into estimator and to improve the accuracy of pseudo measurements for unmeasured buses. The quality, accuracy, standard deviation and computational time are improved due to combined spatial and temporal correlation and using an efficient direct solution that only has a single iteration for the solution. Three case studies are used in this paper to examine and demonstrate the effectiveness of the proposed technique.**

Index Terms—**Distribution system, state estimation, conditional multivariate complex Gaussian distribution, spatial-temporal correlation, measurement error**

I. INTRODUCTION

POWER system state estimation (SE) has extensively been used for transmission systems operation and control, since its first introduction in 1970 [1-3]. Unlike transmission networks, SE is not commonly applied to distribution networks due to the lack of real measurements [4]. However, with increasing penetration of distributed energy resources (DERs) like rooftop PVs and electric storage systems in distribution networks, an improved form of distribution system state estimation (DSSE) is becoming desirable [5-7]. The early development of DSSE goes back to 1990 when the weighted least square (WLS) algorithm was designed and applied to a distribution system [8-11]. Later in 1996, a DSSE was designed and employed as real time monitoring in distribution management system (DMS) for applications such as: volt/var control considering the impacts of DERs, feeder reconfiguration, battery storage management and protection [12, 13].

High penetration of DERs in distribution network on one hand, and unpredictable customer loads behavior on the other hand require fast and accurate DSSE methods for online generation and load demand considerations and planning. However, a high number of customer loads and a huge amount of measured data from smart meters make centralized DSSE algorithms complicated with long processing time [14]. Therefore, an enhanced form of DSSE with significant reduction in measurement points, while retaining accurate estimations, can be an attractive alternative. Generally, decreasing the number of measurement points leads to the under-determined system, which means the measurements cannot provide enough information for the state estimation algorithm [15]. This problem can be resolved using pseudo measurements for unmeasured buses, satisfying the distribution network observability conditions [10]. Pseudo measurements can be obtained from advanced metering infrastructure (AMI), historical data or customers' billing data [16], or they can be calculated based on the nominal customers' load power, consumed power and load profiles in twenty four hours [9]. In the case, when the load in presence of renewable resources the loads do not follow a normal distribution, a Gaussian mixture model with a combination of several normal distributions can represent the load probability density function (PDF) [17]. Although the use of pseudo measurement is becoming an essential part of the DSSE algorithm, the associated error with this type of measurement data is substantial, which can reduce the accuracy and the reliability of the DSSE. This issue can be addressed by considering the spatial correlation between measured and unmeasured points. The impact of correlation between real and pseudo measured data is addressed in [18]. In [19] spatial correlation between loads are used to further increase the accuracy of the estimated PDF of the injected currents in unmeasured buses. In another article, [20] proposed a new method based on artificial neural network (ANN) to train two systems for updating the active and reactive power pseudo measured data based on load profiles, offline power flow analysis and a limited number of real measurement points. ANN is also employed in [21, 22] to model a close loop feedback for continuously monitoring and updating pseudo measured data.

In some of the noted published studies, the spatial correlation is considered, while the impact of temporal correlation is not well addressed in state estimation articles. The temporal correlation represents the fluctuations of measured data according to time, which can further enhance state estimation or forecasting methods accuracy. For instance, in [23] the spatial and temporal correlation of PV power generations are modelled and multivariate predictive distribution of PV power generation is characterized. The generated multivariate predictive distributions describe interdependent generators in contiguous locations. Also, spatial-temporal correlation is considered for load growth forecasting and load demand for Electrical Vehicles (EVs) battery charging in [24, 25]. A new forecasting method is presented in [26], which uses a

generalized maximum likelihood estimator to forecast the states of the system, not only considering the characteristic of loads and DERs but also by integrating the spatial and temporal correlation between them. The correlation between DERs and loads are modelled by a first order Vector Auto-Regressive (VAR) model. VAR model is considered in [27] to integrate time and space correlation of existing measured data for a DSSE algorithm. In [28], spatial-temporal correlation is considered in a Yule-Walker model to forecast the nodal voltage angles. In [28], the authors noted that if the system is in a quasi-steady state, the nodal voltage angles are strongly correlated in time, and the short term forecasting is not necessary. As noted before, the large amount of required data in a distribution network makes the estimation process computationally time consuming, while active distribution networks in presence of DERs require fast and accurate state estimators, updating in less than one second [29]. To deal with the large amount of measured data a new algorithm based on compressed measurements is proposed in [30]. However, employing iterative DSSE algorithm in this article is not time efficient. Consequently, this paper proposes a direct solution with only one iteration state estimation that can be employed for real time studies including; operational control and protection designs and testing algorithms for distribution networks, with the following main contributions:

- Conditional Multivariate Complex Gaussian Distribution (CMCGD) is used to integrate spatial-temporal correlation to estimate all network states including bus voltages, branch currents and injected node currents in one iteration.
- A combined spatial-temporal correlation is included as part of the proposed method to increase the number of corrective terms, significantly improving the accuracy of statistical parameters used through pseudo measurements.
- Correlation indices are analyzed considering number of loads, time intervals, and DER penetration.

This paper is organized as follow: Section II presents the impact of number of customers, type of application and PV penetration on spatial-temporal correlation. The formulation of CMCGD based on spatial-temporal correlation is represented in section III. In section IV the proposed method is applied on three distinct cases to evaluate the effectiveness of the proposed method. Finally, concluding remarks based on the simulation results are stated in the last section.

II. SPATIAL AND TEMPORAL CORRELATION

Correlation is a statistical relationship between two variables which can be represented in time and space. Spatial correlation is computed based on the data form in different locations, while temporal correlation represents the dependency of data based on time [31]. The temporal and spatial correlation are usually defined mathematically as follows [32]:

$$\begin{cases} Correlation_{Spatial} = {cov(x,y)}\big/{\sigma_x * \sigma_y} \\ Correlation_{Temporal} = {cov(x_t, x_{t+n})}\big/{var(x)} \end{cases} \quad (1)$$

where cov, σ and var show covariance, standard deviation and

variance, respectively. In spatial correlation x and y represent two sets of data from different geographic locations, while in temporal correlation the time dependency is also included, i.e. at a given position and time x and t and between different time interval $t + n$. The process of calculating correlation is explained in [32], showing that the type and the location of loads are key factors in the calculating process.

Consequently, the correlation between loads on different buses in a distribution system depends on three other important factors:

1. The number of loads, contributed to load buses,
2. Time interval for which load data is averagely available,
3. DER penetration at load buses.

In order to examine the effect of the first factor, the number of loads on two load buses are incrementally increased, and the correlations is computed as shown in Fig. 1. In order to study the spatial and temporal correlation, the one-minute active power data belonging to one hundred fifty households of real data from Newmarket suburb, Brisbane, Australia are utilized.
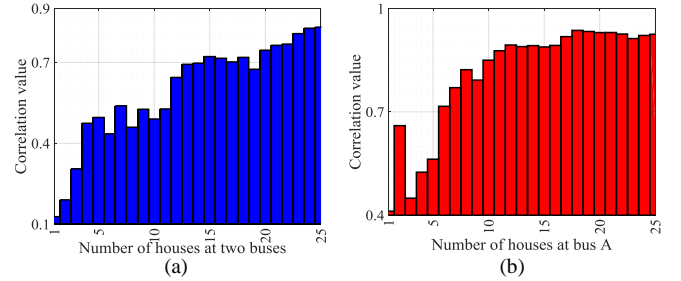

Fig 1. Impact of number of customers on (a) Spatial correlation, (b) Temporal correlation.

As shown in Fig. 1, it is clear that by increasing the number of loads on each bus, the pattern of active powers changes so that load buses become more correlated. As seen in Fig.1 (a), the spatial correlation between two individual houses is 12% while it increases to 83% for twenty-five houses at each bus. In addition, the temporal correlation in Fig. 1 (b) shows the same characteristic that is increasing from 41% for one house to 92% for twenty-five houses at each bus. The jump with two houses in Fig. 1 (b) is by coincident from the data and does not imply to be a general trend.
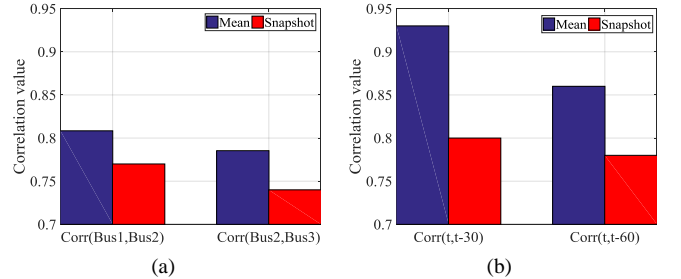

Fig 2. Impact of mean and snapshot values on (a) Spatial correlation, (b) Temporal correlation.

The second statement is the time interval of available data. Some applications require the correlation calculation between loads' average values over longer time intervals. Whereas other algorithms are using the correlation of snapshot values.
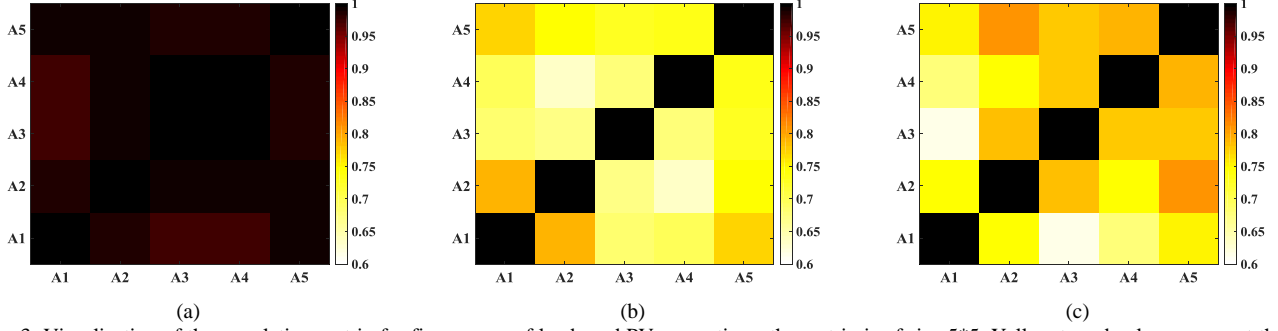
Fig. 3: Visualization of the correlation matrix for five groups of loads and PV generations, the matrix is of size 5*5. Yellow to red colors represent the highest to lowest correlation (a) PV outputs correlation, (b) customer loads correlation, (c) net loads correlation.

In order to show the impact of time interval, three sample load buses, each with twenty households are considered. Fig. 2 (a) shows the spatial correlation between load bus 1 and other two buses, for two time intervals of thirty minutes (Snapshot) and half an hour (Mean of thirty one minute samples). The load data for half an hour time interval obtained by averaging 30 one-minute data. As seen, the spatial correlation has changed slightly, for example from 0.77 to 0.80 for one minute and half an hour time intervals, between bus 1 and 2. However, as depicted in Fig. 2 (b), the temporal correlation between time t and thirty minutes earlier as opposed to sixty minutes before t has increased by almost 10% with half an hour average data which is remarkable improvement.

The last important statement is the DER penetration at load buses. To show this effect, five residential areas with different level of PV penetration are considered. Fig. 3 (a) provides the visualization of the correlation between PV outputs. Close proximity PV generators in distribution networks are highly correlated [23], while this factor for customer loads are near 0.7, as seen in Fig. 3 (b). Consequently, the correlation of net loads is close to that for customer loads, as depicted in Fig. 3 (c). In general, the correlation of net load is close to the minimum of load or generation correlation.

III. SPATIAL-TEMPORAL DISTRIBUTION STATE ESTIMATION: BASICS AND FORMULATION

The aim of designing the proposed DSSE is to improve the accuracy of pseudo measured data based on the spatial-temporal dependency, while simultaneously estimating states in one iteration. Here, CMCGD with built-in spatial-temporal correlation is proposed for DSSE.

A. Conditional Multivariate Complex Gaussian Distribution

There are three parameters representing the Multivariate Complex Gaussian Distribution (MCGD), which are the mean value (μ), covariance matrix (Γ) and pseudocovariance (C) matrix, detailed in [33]. Γ and C for two sets of variables, i.e. 1 and 2 are as in (2):

$$\Gamma = \begin{matrix} \mu_1\{ \\ \mu_2\{ \end{matrix} \begin{bmatrix} \widetilde{\Gamma_{11}} & \widetilde{\Gamma_{12}} \\ \Gamma_{21} & \Gamma_{22} \end{bmatrix}, C = \begin{matrix} \mu_1\{ \\ \mu_2\{ \end{matrix} \begin{bmatrix} \widetilde{C_{11}} & \widetilde{C_{12}} \\ C_{21} & C_{22} \end{bmatrix} \quad (2)$$

For updating the statistical parameters of a set of unmeasured data $[\mu, \Gamma, C]_2$ based on the parameters of measured data $[\mu, \Gamma, C]_1$, the CMCGD formulation in (3) is employed.

$$\acute{\mu}_2 = \mu_2 + A(\mu_1^M - \mu_1) + B(\mu_1^M - \mu_1)^*$$
$$\acute{\Gamma}_{22} = \Gamma_{22} - A\Gamma_{12}^H - B\Gamma_{12}^H \quad (3)$$
$$\acute{C}_{22} = C_{22} - AC_{12}^T - BC_{12}^T$$

where $(.)^*$ is the conjugate operation, μ_1^M is the measured μ_1, $\acute{\mu}_2$, $\acute{\Gamma}_{22}$ and $\acute{C}_{22}$ are the updated of mean, covariance and pseudocovariance matrices of the unmeasured data and A and B are the function of covariance and pseudocovariance matrices [34]. It is worth noting that sometimes the measured data from distribution network with DERs cannot be represented by one normal distribution. Hence, Mixed Gaussian Model can be used to model the data, using some similar Gaussian models [17]. Consequently, the components of each Gaussian are updated based on the proposed state estimation method.

B. DSSE Formulation

A state estimation algorithm such as WLS considers minimization of the error between the measured data (z) and a function ($h(x)$) representing the relation between states (x) and the real measurements $(z = h(x))$, to estimate states [35]. Usually, in this method the states are bus voltage magnitudes and angles, while the measured values are active and reactive power injections/flow power and bus voltages. WLS employs iterative algorithm to estimate states, while the proposed method in this paper is a non-iterative algorithm using a direct solution to estimate the states of the network such as injected/branch currents and bus voltages in one iteration. In the proposed method, the real measured data is from PMUs, whereas pseudo data are generated based on historical data, represented as injected currents (i_{inj}) to estimate bus voltages (v_{inj}) and branch currents (i_{branch}) as well as improving SD of pseudo measurements themselves. System states are related to each other using a direct power flow algorithm, as in (4):

$$\begin{cases} v_{inj} = DLF \times i_{inj} + v_1 \\ i_{branch} = BIBC \times i_{inj} \end{cases} \quad (4)$$

where DLF matrix is the direct load flow matrix and $BIBC$ is the bus-injection to branch-current matrix. These matrices represent the network connection using line impedance, where details are given in [36]. Consequently, based on equations (4) the network states can directly be estimated by (5):

$$\begin{bmatrix} i_{inj} \\ i_{branch} \\ v_{inj} \end{bmatrix} = \begin{bmatrix} I_{n-1} & 0 & 0 \\ 0 & BIBC & 0 \\ 0 & 0 & -DLF \end{bmatrix} \begin{bmatrix} i_{inj} \\ i_{inj} \\ i_{inj} \end{bmatrix} + \begin{bmatrix} 0 \\ 0 \\ v_1 \end{bmatrix} \quad (5)$$

where; I_{n-1} is a unity square matrix with *(n-1)* by *(n-1)* dimension, and *n* is the number of buses.

In this paper, the correlation between customer loads in different geographical locations and temporal correlations between time steps are considered in the DSSE formulations, simultaneously in Γ and C. For estimating complex states, the correlation matrix (CR) contains the relation between active powers $(CR_{PP_{t...(t-n)}})$, active and reactive powers, $(CR_{PQ_{t...(t-n)}})$ and $(CR_{QP_{t...(t-n)}})$, and reactive powers $(CR_{QQ_{t...(t-n)}})$ for different locations and several time steps $(t...(t-n))$ as represented in (6).

$$CR = \begin{bmatrix} CR_{PP_{t...(t-n)}} & CR_{PQ_{t...(t-n)}} \\ CR_{QP_{t...(t-n)}} & CR_{QQ_{t...(t-n)}} \end{bmatrix} \tag{6}$$

Based on these formulations, the following procedure is applied in this paper to implement DSSE algorithm:

1. The required input data includes pseudo and real measurement data, the calculated spatial-temporal correlation matrix based on (1) and (6) and the network schematics and line impedances to calculate BIBC and DLF matrices.

2. Calculate the mean and SD of the real and imaginary part of every load injected currents. The mean value of the injected currents is calculated directly from the historical data using active and reactive power. It is assumed that the injected currents are calculated with respect to the voltage angle of the reference bus. However, the obtained voltage angle from power flow based on the pseudo measurement data, or the angle of the nearest measurement point can be considered as the voltage angle of each bus [37]. The SD of the real and imaginary part of the pseudo measurement data can be calculated based on the mean values and the measurement errors [38].

3. Calculate the covariance between the real and imaginary part of the injected currents based on correlation value and SD using (1) [39].

4. As noted before, the contribution of this paper is to include spatial-temporal correlation in the DSSE algorithm. To integrate spatial-temporal correlation as part of the DSSE algorithm, (5) needs to be revised as in (7):

$$\begin{bmatrix} i_{inj_{n_t}} \\ i_{branch_{n_t}} \\ v_{inj_{n_t}} \end{bmatrix} = \begin{bmatrix} I_{n_t \times (n-1)} & 0 & 0 \\ 0 & BIBC_{n_t} & 0 \\ 0 & 0 & -DLF_{n_t} \end{bmatrix} \begin{bmatrix} i_{inj_{n_t}} \\ i_{inj_{n_t}} \\ i_{inj_{n_t}} \end{bmatrix} + \begin{bmatrix} 0 \\ 0 \\ v_{1_{n_t}} \end{bmatrix} \tag{7}$$

where n_t represents the number of time steps that are considered in DSSE algorithm. $I_{n_t \times (n-1)}$ is an unity matrix and $v_{1_{n_t}}$ is the measured voltage at the reference bus in each time step. $BIBC_{n_t}$ and DLF_{n_t} can be calculated using (8):

$$BIBC_{n_t} = \begin{bmatrix} BIBC & \cdots & 0 \\ 0 & \ddots & 0 \\ 0 & \cdots & BIBC \end{bmatrix}, DLF_{n_t} = \begin{bmatrix} DLF & \cdots & 0 \\ 0 & \ddots & 0 \\ 0 & \cdots & DLF \end{bmatrix} \tag{8}$$

where the number of successive BIBC and DLF in the new matrices is the same as the number of time steps.

5. Consider μ_{i_t} and $\mu_{v_{1_t}}$ are the mean injected currents and voltage at bus 1, in a time step. Now, the mean injected and branch currents and bus voltages (μ_{IBV_t}) are represented as

$$\mu_{IBV_t} = \begin{bmatrix} \mu_{i_t} \\ BIBC_{n_t} * \mu_{i_t} \\ -DLF_{n_t} * \mu_{i_t} + \mu_{v_{1_t}} \end{bmatrix} \tag{9}$$

where *IBV* stands for injected/branch currents/voltage of the buses, and i is the number of bus.

6. Based on the matrices $BIBC_{n_t}$ and DLF_{n_t}, the covariance (Γ_{IBV} and C_{IBV}) matrices, representing the statistical behavior of all the states of the network and for all time steps is given as in (10).

Γ_{IBV}

$$= \begin{bmatrix} \Gamma_i & \Gamma_i * BIBC_{n_t}^H & -\Gamma_i * DLF_{n_t}^H \\ BIBC_{n_t} * \Gamma_i & BIBC_{n_t} * \Gamma_i * BIBC_{n_t}^H & -BIBC_{n_t} * \Gamma_i * DLF_{n_t}^H \\ DLF_{n_t} * \Gamma_i & -DLF_{n_t} * \Gamma_i * BIBC_{n_t}^H & DLF_{n_t} * \Gamma_i * DLF_{n_t}^H + \Gamma_{v1} \end{bmatrix}$$

C_{IBV}

$$= \begin{bmatrix} C_i & C_i * BIBC_N^T & -C_i * DLF_{n_t}^T \\ BIBC_{n_t} * C_i & BIBC_{n_t} * C_i * BIBC_{n_t}^T & -BIBC_{n_t} * C_i * DLF_{n_t}^T \\ DLF_{n_t} * C_i & -DLF_{n_t} * C_i * BIBC_{n_t}^T & DLF_{n_t} * C_i * DLF_{n_t}^T + C_{v1} \end{bmatrix} \tag{10}$$

7. By considering temporal correlation, equation (3) can be rewritten as:

$$\mu_2' = \mu_2 + \sum_{i=1}^{t} \left[A\left(\mu_1^M(i,) - \mu_1(i,)\right) + B\left(\mu_1^M(i,) - \mu_1(i,)\right)^* \right]$$
$$\Gamma_{22_t}' = \Gamma_{22_t} - A\Gamma_{12_t}^H - B\Gamma_{12_t}^H \tag{11}$$
$$C_{22_t}' = C_{22_t} - AC_{12_t}^T - BC_{12_t}^T$$

where $(,)$ represents an element of the matrix and t in covariance and pseudocovariance matrixes represents pervious time steps in these matrixes. From the summation terms, it can be inferred that the corrective terms are increased by increasing the number of the time steps, which make it plausible that the temporal correlation may decrease the error of the estimated states. However, the measured data at time t is correlated to the several pervious time steps, which means that, increasing the number of imported data may not be effective to increase the accuracy, and can only increase the computation time.

8. After updating the covariance and pseudocovariance matrices using (10), the real ($COV_{Re,Re}$) and imaginary ($COV_{Im,Im}$) part of the covariance between states can be calculated as in (12) [40]:

$$\begin{cases} COV_{Re,Re} = {}^1\!/_2 \, Real(\Gamma_{IBV} + C_{IBV}), \\ COV_{Im,Im} = {}^1\!/_2 \, Real(\Gamma_{IBV} - C_{IBV}) \\ COV_{Re,Im} = {}^1\!/_2 \, Imaginary(\Gamma_{IBV} + C_{IBV}), \\ COV_{Im,Re} = {}^1\!/_2 \, Imaginary(\Gamma_{IBV} - C_{IBV}) \end{cases} \tag{12}$$

9. Finally, based on the results in the previous step the variance (VAR) of the magnitude and angle of the states can be written as in (13).

$$\begin{cases} Var(|X|) = \mu_{X^{RI}}^T * Cov_{X^{RI},X^{RI}} * \mu_{X^{RI}} / \|X^{RI}\|^2 \\ Var(\angle X) = \mu_{X^{IR}}^T * Cov_{X^{RI},X^{RI}} * \mu_{X^{IR}} / \|X^{RI}\|^4 \end{cases} \tag{13}$$

where $X = X^{Re} + jX^{Im}$, $X^{RI} = [X^{Re} \ X^{Im}]^T$, $X^{IR} = [-X^{Im} \ X^{Re}]^T$, $\|X^{RI}\|$ is l_2 norm of X^{RI}, and $Cov_{X^{RI},X^{RI}} = \begin{bmatrix} COV_{Re,Re} & COV_{Re,Im} \\ COV_{Im,Re} & COV_{Im,Im} \end{bmatrix}$.

In order to decrease the computational complexity and simulation time for real time applications, the first four steps can be computed off-line. For bad data detection, the measurement values out of the range ± 3 SD, can be considered as bad data [41].

IV. SIMULATION RESULTS

In this section, three case studies are considered. The first one

is the six bus radial distribution network [36]. In this case study, several operation conditions tested to evaluate the performance of the proposed method. For further study, this algorithm is employed in a larger network such as the 123 node IEEE test feeder [42]. Finally, a distribution network based on the real residential data with PV penetration is studied.

The SD of the states calculated based on the error of the measurement, which turned out to be 3 and 50 percent for real and pseudo measured data, respectively.

It should be noted that the correlation matrix in this study should be positive definite. Therefore, in the cases of real data analysis, Rstudio is employed to find the nearest positive definite correlation matrix[43].

In order to show the effectiveness of the temporal correlation in the proposed CMCGD spatial-temporal (CST) method, the results of the estimated states are compared with CMCGD spatial (CS) model and WLS algorithm. The average voltage error (AVE), computational time, number of the iteration and the quality of the state estimator calculated based on the SD of the estimated states [17], are used for comparison. AVE in case study one and two are the average error of buses at one time, while in case study three represents the average estimated error at each bus for one day. AVE criterion has priority in comparison with other three factors, because the control and protection algorithms consider the bus voltages as the input to their algorithms in choosing the accurate decisions and relevant operation procedures. Computational time and iteration are also playing an important role in control and protection applications.

A. Case Study 1: 6-bus distribution system

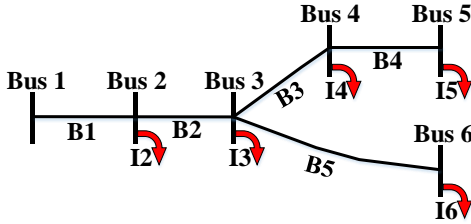Fig. 4 shows a 6-bus radial distribution network.

Fig. 4. A six-bus distribution network.

The pseudo measurement of injected currents on each bus provided in Table I.

TABLE I
PSEUDO MEASURED INJECTED CURRENT AT 100% LOADING CONDITION

Bus number	2	3	4	5	6
Injected current(A)	18.9-6.7i	13.4-12.7i	14.8-10.9i	16.8-14.9i	17.7-14.9i

In order to examine the impact of the correlation between the variables in this study, two types of load groups are considered. The buses 2, 3 and 5 are representing the group of residential loads, while 4 and 6 are a combination of several industrial loads. In a distribution networks, same load types are highly correlated in a time interval. The correlation matrix in case 1 is visualized in Fig. 5, where black to white color shows the highest to lowest correlations. In this case, three scenarios are considered. In the first scenario, only bus number 2 has an injection current measurement, and for other buses, the injected current data considered at 100% loading, as pseudo measurements. In this scenario, as shown on the daily load profile in Fig. 6, the loading of the system decreases in three

steps by; 20, 40 and 60 percent, while DSSE uses 100% magnitudes of pseudo measured data. In order to compare the results of the three methods, i.e. WLS, CS, and CST, four criteria considered as shown in Table II. MATLAB on Intel Core i70-4600 with clock speed 2.7 GHz and 16 GBRAM was used to obtain the results.
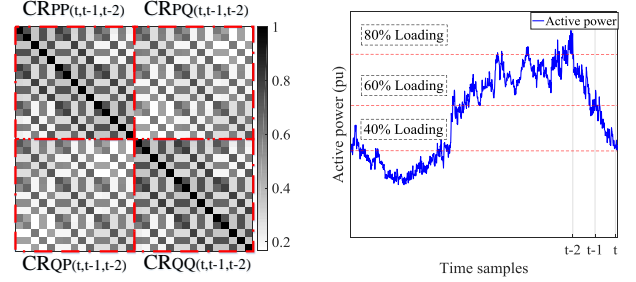

Fig 5. Visualization of correlation matrix.

Fig 6. Operation loading in case study 1.

TABLE II
COMPARISON IN SCENARIO 1 FOR THREE TIME STEPS WITH LOADING DECREASE

	Time step 1: %80 Loading			Time step 2: %60 Loading			Time step 3: %40 Loading		
	WLS	CS	CST	WLS	CS	CST	WLS	CS	CST
AVE (%)	3.9	0.3	0.3	4.8	0.9	0.7	6.1	1.4	1.1
Quality	6.76	7.41	7.41	6.76	7.41	7.42	6.76	7.41	7.42
Time(sec)	0.03	0.01	0.01	0.03	0.01	0.01	0.03	0.01	0.01
Iterations	5	1	1	5	1	1	5	1	1

The loading of bus 2 is updated in WLS algorithm, but the other customer loads and the error of the pseudo measured data are not updated, and still the SD of the estimated states is ~~still~~ higher than other two methods in Table II. Consequently, the quality of the measurement in WLS, which is 6.76, is lower than the other two methods, while by updating the SD of the estimated states, this index for the other two methods become 7.41 and 7.42. The number of iteration may increase the simulation time, give rise to 0.03 second computation time in WLS algorithm. However, the computational time in the other two methods is 0.01 second. In the first time step, the load level is 80% and only one new measured data is imported into the algorithms. Hence, the temporal correlation cannot be considered here and the output of CS and CST are the same. The AVE in WLS is 3.9% while this index is 0.3% for both other two methods in the first time step. This difference is because of the fact that in WLS algorithm, the statistical parameters of pseudo measurements are not updated based on the measured input. For the next time step, the system operates at 60% loading, in which the loading of bus number 2 is updated in all algorithms. Additionally, the pervious measured value is kept in CST algorithm. By reducing the loading of the system to 60%, the difference between available pseudo data to the estimator (100% loading) and the real measurement is increased, which causes a rise in the error of WLS to 0.9%. As seen in Table II, the AVE in CST is 0.7%, which is lower than 0.9% for CS. By importing two measured data from two time steps in CST, based on (11), the error of the estimated states in CST becomes lower than CS. In the last time step of the first scenario, the 6-bus system is operating at 40%loading. Again, the measured data in the last two time steps are kept the same for CST. As expected, the average error in WLS is increased to

6.1%. This error is 1.4% and 1.1% for CS and CST, respectively, which shows the effectiveness of employing temporal and spatial correlation into the design for state estimation algorithm. Fig. 7 (a) shows the AVE in the first scenario. It is obvious that by increasing the difference between pseudo measured value and the real measurements, the estimated states errors increases considerably. However, the error of CST is less than those for the two other methods, providing a better accuracy with the same number of measurements

In the second scenario, the loading levels are 80% and 40% in the first two steps and then 60% in the last step. In this scenario, the impact of system load decrease and increase is studied. As shown in Fig. 7 (b), the CST algorithm is more effective in this scenario as well, compared to other algorithms. As seen in Table III, the average voltage error for 40% and 60% loading are decreased to 1.2% and 0.5%, respectively. While, these errors are 1.4% and 0.9% in CS algorithm and 6.1% and 4.8% in WLS algorithm for the first and second time steps, respectively. Furthermore, the impact of considering more time steps is shown here. For instance, in the first scenario, AVE at 60% loading in the second time step is 0.7%, while by adding one more measured data in the second scenario this error is decreased to 0.5% in the third time step.

TABLE III
COMPARISON IN SCENARIO 2 FOR THREE TIME STEPS WITH LOADING DECREASE AND INCREASE

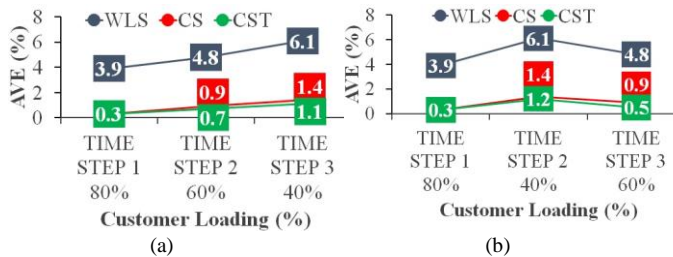|	Time step 1: %80 Loading			Time step 2: %40 Loading			Time step 3: %60 Loading		
	WLS	CS	CST	WLS	CS	CST	WLS	CS	CST
AVE (%)	3.9	0.3	0.3	6.1	1.4	1.2	4.8	0.9	0.5
Quality	6.76	7.41	7.41	6.76	7.41	7.42	6.76	7.41	7.42
Time(sec)	0.03	0.01	0.01	0.03	0.01	0.01	0.03	0.01	0.01
Iterations	5	1	1	5	1	1	5	1	1

Fig. 7. AVE for (a) Scenario 1, (b) Scenario 2.

As noted before, two different load types are considered in the first case study, which are not highly correlated. In the third scenario, another measured device is considered on the industrial load group on bus number 4. The aim of this case study is to show that by spatially distributed measurement points, the error will be decreased significantly. Table IV illustrates the results of the simulation for three time steps. As shown in Fig 8, by adding another measurement point to WLS algorithm, the error is decreased slightly, because in this method, the load group correlation is not considered. However, the impact of considering another measured device on one of the industrial load group is obviously remarkable in CS and CST. In CS method the error in the first scenario is 0.3, 0.9 and 1.4 percent, respectively, while by importing a new measured data on bus 4, errors are decreased to 0.1, 0.4 and 0.8. CST has

the same pattern like CS. However, in three steps the error of estimated voltages is decreased to 0.1, 0.3 and 0.6 percent, respectively using the proposed CST algorithm.
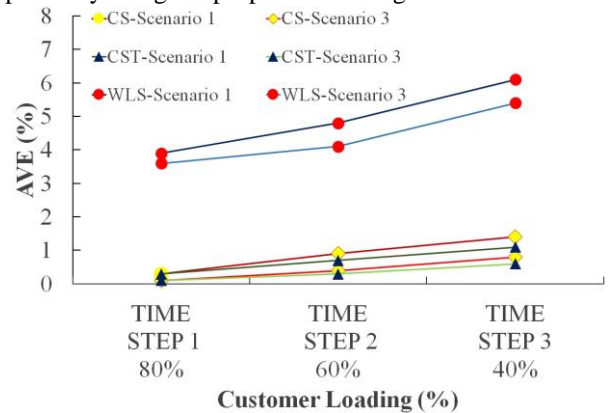

Fig. 8. Average voltage error at scenario 1 and 3.

TABLE IV
COMPARISON IN SCENARIO 3 CONSIDERING TWO MEASUREMENT POINTS FOR THREE TIME STEPS

	Time step 1: %80 Loading			Time step 2: %60 Loading			Time step 3: %40 Loading		
	WLS	CS	CST	WLS	CS	CST	WLS	CS	CST
AVE (%)	3.6	0.1	0.1	4.1	0.4	0.3	5.4	0.7	0.6
Quality	6.78	7.42	7.42	6.81	7.42	7.42	6.81	7.42	7.42
Time(sec)	0.03	0.01	0.01	0.03	0.01	0.01	0.03	0.01	0.01
Iterations	5	1	1	5	1	1	5	1	1

B. Case Study 2: IEEE 123 node test feeder

In order to show the performance of the proposed method in a larger distribution network, IEEE 123 node test feeder is considered in this case study as shown in Fig 9. The load data in [44] is employed as pseudo measured data as 100% loading of this network. The blue area shows the group of residential loads, while the green areas are three industrial states. Then, the correlation matrix is formed with the correlation coefficients as in the first case study. In the second case study, six measurement points are assumed from which one measurement points is considered for each industrial area, installed on buses 28, 77 and 109. Also, for residential loads three measurement points are considered on buses 2, 48 and 69. Three operating load point of 80%, 60% and 40% in three time steps are studied in this case. Table V shows the results for the three algorithms in each time steps.
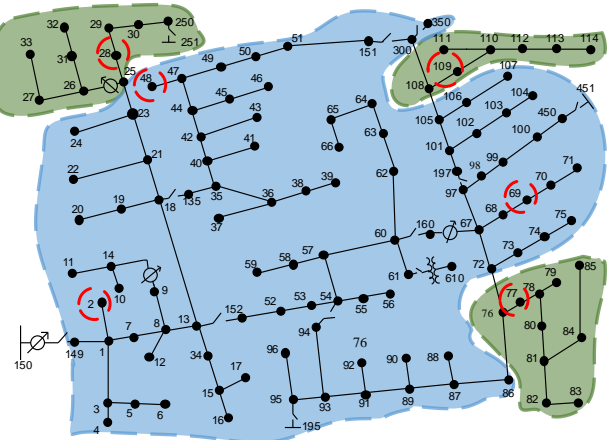

Fig. 9. IEEE 123 node test feeder [44].

As noted before, in the first simulation, only one measured set of data is available, the results for both CS and CST method are the same. As seen, the computational performance of WLS is low with the running time of 0.12 compared with 0.04 second of the other two algorithms. As expected, by increasing the number of the buses, the quality of the state estimation is decreased and reaches to 2.33, 4.48 and 4.48 for WLS, CS and CST, respectively. Furthermore, the AVE for WLS is around 2% while it is 0.09% for CS and CST. In the second and third time steps, the loading of the distribution network is 60% and 40%. In these time steps, the error is increased for all three algorithms; however, the CST has the lowest error due to using both spatial and temporal correlations among measured data in three time steps. The simulation running time in CST is increased due to the fact that the amount of imported data to this algorithm is three times larger than the CS algorithm. The simulation time difference between these two methods is around 0.03 second that can be managed in the application of state estimation in distribution networks.

TABLE V
COMPARISON IN CASE STUDY 2 FOR THREE LOAD DECREASING STEPS

	Time step 1: %80 Loading			Time step 2: %60 Loading			Time step 3: %40 Loading		
	WLS	CS	CST	WLS	CS	CST	WLS	CS	CST
AVE (%)	2.05	0.09	0.09	2.45	0.32	0.3	2.84	0.52	0.42
Quality	2.33	4.48	4.48	2.42	4.48	4.48	2.42	4.48	4.49
Time(sec)	0.12	0.04	0.04	0.12	0.04	0.05	0.12	0.04	0.07
Iterations	5	1	1	5	1	1	5	1	1

C. Case Study 3

In the third case study, the proposed method is applied to a residential network with PV as shown in Fig. 10.
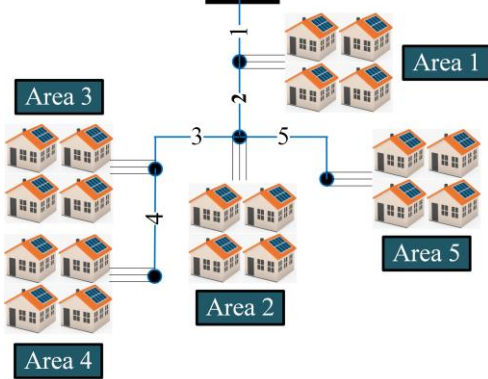

Fig. 10. Schematic of residential distribution network.

The residential and PV data from real measurements located in Newmarket suburb, Brisbane, Australia is used for this case study. The load and PV data grouped for five areas, while area 1 has the real measurement.

Fig. 11 shows the effectiveness of the proposed method for this network. The period that PV power is injected to the network is shown on Fig 11 with red dashed lines. In addition to AVE, maximum voltage error (MVE) is also considered to compare the performance of three state estimators in dynamic study as shown in Table VI. The high spatial-temporal correlation is the reason for reliable performance of CST compared with other two methods in dynamic state estimation. In this study, the maximum AVEs for WLS and CS are 0.75 % and 0.55%, while in CST it is decreased to 0.31%. Also, the

maximum MVE for one day state estimating with CST algorithm is around 1.4%, which is less than 2% and 1.9 % with WLS and CS methods. It is worth noting, the inclusion of PV is expected to decrease the accuracy of DSE. However, the underlying correlation formulation [34] used in this paper together with load and PV grouping procedure would enable updating the net loads of the other areas by using equation (11). This procedure increases the accuracy of pseudo measured data in unmeasured areas.

TABLE VI
COMPARISON IN CASE STUDY 3 FOR ONE DAY

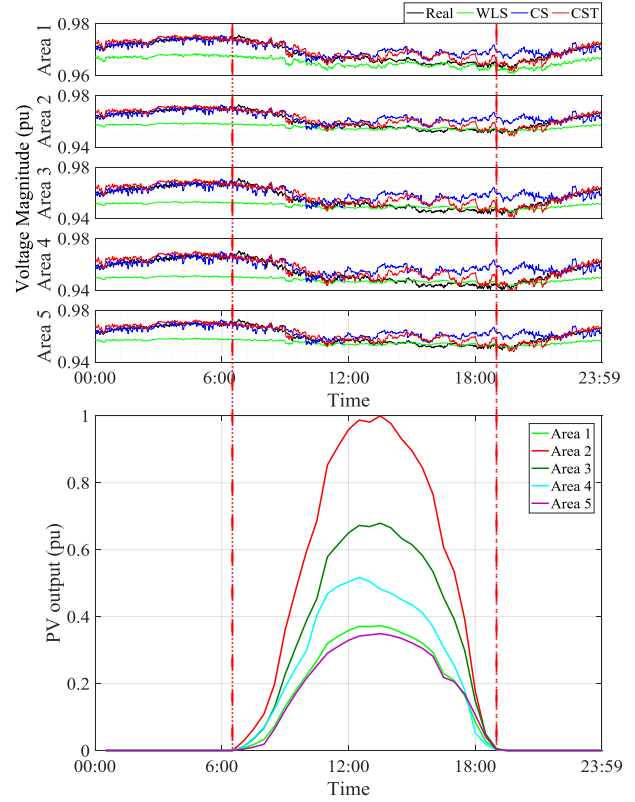|	WLS		CS		CST	
	AVE(%)	MVE(%)	AVE(%)	MVE(%)	AVE(%)	MVE(%)
Area 1	0.37	0.80	0.19	0.72	0.11	0.51
Area 2	0.57	1.5	0.38	1.4	0.22	0.97
Area 3	0.69	1.9	0.50	1.8	0.30	1.3
Area 4	0.73	2.0	0.55	1.9	0.31	1.4
Area 5	0.57	1.5	0.39	1.5	0.23	1.0

Fig. 11. Voltage magnitude and PV generations in the third case

V. CONCLUSION

This paper proposes an efficient direct state estimation method to estimate node voltages, branch currents, and injection currents in distribution networks with renewable resources. The proposed technique considers spatial and temporal correlation based on conditional multivariate complex Gaussian distribution. This method requires only a few real measurements, which significantly reduces hardware measuring devices. The proposed estimator is very efficient and provides results in one computational operation without the need for the iterative procedure. Three case studies were used to examine the proposed method. The results in all three case studies indicate the accuracy and the effectiveness of the proposed technique in this paper.

REFERENCES

[1] F. C. Schweppe and J. Wildes, "Power system static-state estimation, Part I: Exact model," *IEEE Transactions on Power Apparatus and Systems,* pp. 120-125, 1970.

[2] F. C. Schweppe and D. B. Rom, "Power system static-state estimation, Part II: Approximate model," *power apparatus and systems, IEEE Transactions on,* pp. 125-130, 1970.

[3] F. Schweepe, "Power System Static State Estimation, Part III: Implementation," ed: *IEEE Transaction on Power Apparatus and Systems*, 1970.

[4] M. L. Kumar, H. M. Prasanna, and T. Ananthapadmanabha, "RETRACTED: A Literature Review on Distribution System State Estimation," *Procedia Technology,* vol. 21, pp. 423-429, 2015.

[5] A. Ranković, B. M. Maksimović, and A. T. Sarić, "A three-phase state estimation in active distribution networks," *International Journal of Electrical Power & Energy Systems,* vol. 54, pp. 154-162, 2014.

[6] A. S. Meliopoulos, G. J. Cokkinides, R. Huang, E. Farantatos, S. Choi, Y. Lee*, et al.*, "Smart Grid Technologies for Autonomous Operation and Control," *IEEE Transaction on Smart Grid,* vol. 2, pp. 1-10, 2011.

[7] G. T. Heydt, "The next generation of power distribution systems," *IEEE Transactions on Smart Grid,* vol. 1, pp. 225-235, 2010.

[8] C. Lu, J. Teng, and W.-H. Liu, "Distribution system state estimation," *IEEE Transactions on Power Systems,* vol. 10, pp. 229-240, 1995.

[9] I. Roytelman and S. Shahidehpour, "State estimation for electric power distribution systems in quasi real-time conditions," *IEEE Transactions on Power Delivery,* vol. 8, pp. 2009-2015, 1993.

[10] M. E. Baran and A. W. Kelley, "State estimation for real-time monitoring of distribution systems," *IEEE Transactions on Power Systems,* vol. 9, pp. 1601-1609, 1994.

[11] W.-M. Lin and J.-H. Teng, "Distribution fast decoupled state estimation by measurement pairing," *IEE Proceedings-Generation, Transmission and Distribution,* vol. 143, pp. 43-48, 1996.

[12] A. Primadianto and C.-N. Lu, "A Review on Distribution System State Estimation," *IEEE Transactions on Power Systems,* 2016.

[13] Y. Zhang, X. Du, and M. Salman, "Battery state estimation with a self-evolving electrochemical ageing model," *International Journal of Electrical Power & Energy Systems,* vol. 85, pp. 178-189, 2017.

[14] X. Qing, H. R. Karimi, Y. Niu, and X. Wang, "Decentralized unscented Kalman filter based on a consensus algorithm for multi-area dynamic state estimation in power systems," *International Journal of Electrical Power & Energy Systems,* vol. 65, pp. 26-33, 2015.

[15] O. Krause, D. Martin, and S. Lehnhoff, "Under-determined WLMS state estimation," in *Power and Energy Engineering Conference (APPEEC), 2015 IEEE PES Asia-Pacific*, 2015, pp. 1-6.

[16] A. K. Ghosh, D. L. Lubkeman, M. J. Downey, and R. H. Jones, "Distribution circuit state estimation using a probabilistic approach," *IEEE Transactions on Power Systems,* vol. 12, pp. 45-51, 1997.

[17] R. Singh, B. Pal, and R. Jabr, "Distribution system state estimation through Gaussian mixture model of the load as pseudo-measurement," *IET generation, transmission & distribution,* vol. 4, pp. 50-59, 2010.

[18] C. Muscas, M. Pau, P. A. Pegoraro, and S. Sulis, "Effects of measurements and pseudomeasurements correlation in distribution system state estimation," *IEEE Transactions on Instrumentation and Measurement,* vol. 63, pp. 2813-2823, 2014.

[19] G. Valverde, A. T. Saric, and V. Terzija, "Stochastic monitoring of distribution networks including correlated input variables," *IEEE Transactions on Power Delivery,* vol. 28, pp. 246-255, 2013.

[20] E. Manitsas, R. Singh, B. C. Pal, and G. Strbac, "Distribution system state estimation using an artificial neural network approach for pseudo measurement modeling," *IEEE Transactions on Power Systems,* vol. 27, pp. 1888-1896, 2012.

[21] J. Wu, Y. He, and N. Jenkins, "A robust state estimator for medium voltage distribution networks," *IEEE Transactions on Power Systems,* vol. 28, pp. 1008-1016, 2013.

[22] B. P. Hayes, J. K. Gruber, and M. Prodanovic, "A closed-loop state estimation tool for MV network monitoring and operation," *IEEE Transactions on Smart Grid,* vol. 6, pp. 2116-2125, 2015.

[23] F. Golestaneh, H. B. Gooi, and P. Pinson, "Generation and evaluation of space–time trajectories of photovoltaic power," *Applied Energy,* vol. 176, pp. 80-91, 2016.

[24] J. D. Melo, E. M. Carreno, and A. Padilha-Feltrin, "Spatial-temporal simulation to estimate the load demand of battery electric vehicles charging in small residential areas," *Journal of Control, Automation and Electrical Systems,* vol. 25, pp. 470-480, 2014.

[25] J. D. Melo, E. M. Carreno, and A. Padilha-Feltrin, "Estimation of a preference map of new consumers for spatial load forecasting simulation methods using a spatial analysis of points," *International Journal of Electrical Power & Energy Systems,* vol. 67, pp. 299-305, 2015.

[26] J. Zhao, G. Zhang, Z. Y. Dong, and M. La Scala, "Robust forecasting aided power system state estimation considering state correlations," *IEEE Transactions on Smart Grid,* 2016.

[27] Y. Chakhchoukh, V. Vittal, and G. T. Heydt, "PMU based state estimation by integrating correlation," *IEEE Transactions on Power Systems,* vol. 29, pp. 617-626, 2014.

[28] M. Hassanzadeh, C. Y. Evrenosoğlu, and L. Mili, "A short-term nodal voltage phasor forecasting method using temporal and spatial correlation," *IEEE Transactions on Power Systems,* vol. 31, pp. 3881-3890, 2016.

[29] A. Primadianto and C.-N. Lu, "A review on distribution system state estimation," *IEEE Transactions on Power Systems,* vol. 32, pp. 3875-3883, 2017.

[30] S. S. Alam, B. Natarajan, and A. Pahwa, "Distribution grid state estimation from compressed measurements," *IEEE Transactions on Smart Grid,* vol. 5, pp. 1631-1642, 2014.

[31] J. F. Buford, X. Wu, and V. Krishnaswamy, "Spatial-temporal event correlation," in *Communications, 2009. ICC'09. IEEE International Conference on*, 2009, pp. 1-6.

[32] J. Lee Rodgers and W. A. Nicewander, "Thirteen ways to look at the correlation coefficient," *The American Statistician,* vol. 42, pp. 59-66, 1988.

[33] S. Kanna, D. H. Dini, Y. Xia, S. Hui, and D. P. Mandic, "Distributed widely linear Kalman filtering for frequency estimation in power networks," *IEEE Transactions on Signal and Information Processing over Networks,* vol. 1, pp. 45-57, 2015.

[34] B. Picinbono, "Second-order complex random vectors and normal distributions," *IEEE Transactions on Signal Processing,* vol. 44, pp. 2637-2640, 1996.

[35] A. Abur and A. G. Exposito, *Power system state estimation: theory and implementation*: CRC press, 2004.

[36] J.-H. Teng, "A direct approach for distribution system load flow solutions," *IEEE Transactions on Power Delivery,* vol. 18, pp. 882-887, 2003.

[37] D. A. Haughton and G. T. Heydt, "A linear state estimation formulation for smart distribution systems," *IEEE Transactions on Power Systems,* vol. 28, pp. 1187-1195, 2013.

[38] C. Muscas, F. Pilo, G. Pisano, and S. Sulis, "Optimal allocation of multichannel measurement devices for distribution state estimation," *IEEE Transactions on Instrumentation and Measurement,* vol. 58, pp. 1929-1937, 2009.

[39] P. J. Schreier and L. L. Scharf, *Statistical signal processing of complex-valued data: the theory of improper and noncircular signals*: Cambridge University Press, 2010.

[40] S. L. Goh and D. P. Mandic, "An augmented extended Kalman filter algorithm for complex-valued recurrent neural networks," *Neural Computation,* vol. 19, pp. 1039-1055, 2007.

[41] A. Arefi, G. Ledwich, and B. Behi, "An efficient DSE using conditional multivariate complex Gaussian distribution," *IEEE Transactions on Smart Grid,* vol. 6, pp. 2147-2156, 2015.

[42] Z. Liu, F. Wen, and G. Ledwich, "Optimal planning of electric-vehicle charging stations in distribution systems," *IEEE Transactions on Power Delivery,* vol. 28, pp. 102-110, 2013.

[43] D. Bates and M. Maechler, "R package Matrix: Sparse and dense matrix classes and methods," ed, 2013.

[44] D. T. Feeders, "IEEE PES Distribution System Analysis Subcommittee's, Distribution Test Feeder Working Group," ed: ed, 2013.